

${}^4\text{He} + n + n$ Continuum within an *Ab initio* Framework

Carolina Romero-Redondo,^{1,*} Sofia Quaglioni,^{2,†} Petr Navrátil,^{1,‡} and Guillaume Hupin^{2,§}

¹TRIUMF, 4004 Wesbrook Mall, Vancouver, British Columbia V6T 2A3, Canada

²Lawrence Livermore National Laboratory, P.O. Box 808, L-414, Livermore, California 94551, USA

(Received 4 April 2014; published 16 July 2014)

The low-lying continuum spectrum of the ${}^6\text{He}$ nucleus is investigated for the first time within an *ab initio* framework that encompasses the ${}^4\text{He} + n + n$ three-cluster dynamics characterizing its lowest decay channel. This is achieved through an extension of the no-core shell model combined with the resonating-group method, in which energy-independent nonlocal interactions among three nuclear fragments can be calculated microscopically, starting from realistic nucleon-nucleon interactions and consistent *ab initio* many-body wave functions of the clusters. The three-cluster Schrödinger equation is solved with three-body scattering boundary conditions by means of the hyperspherical-harmonics method on a Lagrange mesh. Using a soft similarity-renormalization-group evolved chiral nucleon-nucleon potential, we find the known $J^\pi = 2^+$ resonance as well as a result consistent with a new low-lying second 2^+ resonance recently observed at GANIL at 2.6 MeV above the ${}^6\text{He}$ ground state. We also find resonances in the 2^- , 1^+ , and 0^- channels, while no low-lying resonances are present in the 0^+ and 1^- channels.

DOI: 10.1103/PhysRevLett.113.032503

PACS numbers: 21.60.De, 25.10.+s, 27.20.+n

Introduction.—Nuclear systems near the drip lines, the limits of the nuclear chart beyond which neutrons or protons start dripping out of nuclei, offer an exciting opportunity to advance our current understanding of the interactions among nucleons, so far mostly based on the study of stable nuclei. This is not a goal devoid of challenges. Experimentally, the study of these rare nuclei with atypical neutron-to-proton ratios is challenged by their short half-lives and minute production cross sections. A major stumbling block in nuclear theory has to deal with the low breakup thresholds, which cause bound, resonant, and scattering states to be strongly coupled. Particularly arduous, in this respect, are those systems for which the lowest threshold for particle emission is of the three-body nature, such as ${}^6\text{He}$, which breaks into an α particle (${}^4\text{He}$ nucleus) and two neutrons at the excitation energy of 0.975 MeV. Aside from a narrow resonance characterized by spin parity $J^\pi = 2^+$, located at 1.8 MeV above the ground state (g.s.), the positions, spins, and parities of the excited states of this nucleus are still under discussion. Experimentally, the picture is not clear. Proton-neutron exchange reactions between two fast colliding nuclei produced resonantlike structures around 4 [1] and 5.6 [2] MeV of widths $\Gamma \sim 4$ and 10.9 MeV, respectively, as well as a broad asymmetric bump at ~ 5 MeV [3], but disagree on the nature of the underlying ${}^6\text{He}$ excited state(s). While the structures of Refs. [1,3] are explained as dipole excitations compatible with oscillations of the positively charged ${}^4\text{He}$ core against the halo neutrons, that of Ref. [2] is identified as a second 2^+ state. More recently, a much narrower 2^+ ($\Gamma = 1.6$ MeV) state and a $J = 1$ resonance ($\Gamma \sim 2$ MeV) of unassigned parity were populated at 2.6 and 5.3 MeV, respectively, with the two-neutron

transfer reaction ${}^8\text{He}(p, {}^3\text{H}){}^6\text{He}^*$ [4]. On the theory side, several predictions, all incomplete in different ways, suggest a 2_1^+ , 2_2^+ , 1^+ , 0^+ sequence of levels above the first excited state but disagree on the positions and widths. Those from six-body calculations with realistic Hamiltonians [5–7] were obtained within a bound-state approximation and cannot provide any information about the widths of the levels. Vice versa, those from three-body models [8,9], from microscopic three-cluster models [10,11], or from calculations hinging on a shell-model picture with an inert ${}^4\text{He}$ core [12,13] can describe the continuum but were obtained using schematic interactions and a simplified description of the structure. In this Letter, we present the first *ab initio* calculation of the ${}^4\text{He} + n + n$ continuum starting from a nucleon-nucleon (*NN*) interaction that describes two-nucleon properties with high accuracy.

Formalism.—In the no-core shell model combined with the resonating-group method (NCSM/RGM), *A*-body bound and/or scattering states characterized by three-cluster configurations are described by the wave function

$$|\Psi^{JT}\rangle = \sum_{\nu} \iint dx dy x^2 y^2 \hat{\mathcal{A}}_{\nu} |\Phi_{\nu xy}^{JT}\rangle G_{\nu}^{JT}(x, y), \quad (1)$$

in terms of a set of unknown continuous amplitudes $G_{\nu}^{JT}(x, y)$ and (a_1, a_2, a_3) ternary cluster channels

$$\begin{aligned} &|\Phi_{\nu xy}^{JT}\rangle \\ &= \left[(|a_1 \alpha_1 I_1^{\pi_1} T_1\rangle |a_2 \alpha_2 I_2^{\pi_2} T_2\rangle |a_3 \alpha_3 I_3^{\pi_3} T_3\rangle \right)_{(s_{23} T_{23})} \right]^{(ST)} \\ &\times (Y_{\ell_x}(\hat{\eta}_{23}) Y_{\ell_y}(\hat{\eta}_{1,23}))^{(L)} \Big]^{(JT)} \frac{\delta(x - \eta_{23})}{x \eta_{23}} \frac{\delta(y - \eta_{1,23})}{y \eta_{1,23}} \quad (2) \end{aligned}$$

built within a translation-invariant harmonic oscillator (HO) basis from NCSM eigenstates of each of the three clusters $|a_1\alpha_1 I_1^{\pi_1} T_1\rangle$, $|a_2\alpha_2 I_2^{\pi_2} T_2\rangle$, and $|a_3\alpha_3 I_3^{\pi_3} T_3\rangle$ and antisymmetrized with an appropriate operator $\hat{\mathcal{A}}_\nu$ to exactly preserve the Pauli exclusion principle. In Eq. (2), a_1 , a_2 , and a_3 (with $a_1 + a_2 + a_3 = A$, and a_1 corresponding to $A - a_{23}$ in Ref. [14]) indicate the mass numbers of the three clusters having angular momentum, parity, isospin, and energy quantum numbers $I_i^{\pi_i} T_i$ and α_i ($i = 1, 2, 3$). Each channel is identified by its total angular momentum, parity, and isospin ($J^{\pi T}$) and an index ν specifying all other quantum numbers, i.e., $\nu = \{a_1\alpha_1 I_1^{\pi_1} T_1; a_2\alpha_2 I_2^{\pi_2} T_2; a_3\alpha_3 I_3^{\pi_3} T_3; s_{23} T_{23} S \ell_x \ell_y L\}$. Further, $\vec{\eta}_{1,23} = \eta_{1,23} \hat{\eta}_{1,23}$ and $\vec{\eta}_{23} = \eta_{23} \hat{\eta}_{23}$ are relative coordinates proportional, respectively, to the displacement between the center of mass (c.m.) of the first cluster and that of the residual two fragments, and to the distance between the c.m.'s of clusters 2 and 3.

The continuous amplitudes $G_\nu^{J^{\pi T}}(x, y)$ are related to the relative motion wave functions among the clusters

$$\begin{aligned} \chi_\nu^{J^{\pi T}}(x, y) &= [\mathcal{N}^{1/2} G]_\nu^{J^{\pi T}}(x, y) \\ &= \frac{1}{\rho^{5/2}} \sum_K u_{\nu K}^{J^{\pi T}}(\rho) \phi_K^{\ell_x \ell_y}(\alpha), \end{aligned} \quad (3)$$

which, introducing the hyperspherical coordinates $\rho = \sqrt{x^2 + y^2}$ and $\alpha = \arctan(x/y)$, can be expanded over the complete set $\phi_K^{\ell_x \ell_y}(\alpha)$, the hyperangular part of the hyperspherical harmonics $\mathcal{Y}_{LM_L}^{\ell_x \ell_y}(\Omega) = \phi_K^{\ell_x \ell_y}(\alpha) (Y_{\ell_x}(\hat{\eta}_{23}) Y_{\ell_y}(\hat{\eta}_{1,23}))_{ML}^{(L)}$. The unknown amplitudes $u_{\nu K}^{J^{\pi T}}(\rho)$ are then found by solving the nonlocal hyper-radial equations

$$\sum_{K\nu} \int d\rho \rho^5 \bar{\mathcal{H}}_{\nu\nu}^{K'K}(\rho', \rho) \frac{u_{\nu K}^{J^{\pi T}}(\rho)}{\rho^{5/2}} = E \frac{u_{\nu K}^{J^{\pi T}}(\rho')}{\rho'^{5/2}}, \quad (4)$$

where $\bar{\mathcal{H}}_{\nu\nu}^{K'K}(\rho', \rho) = [\mathcal{N}^{-1/2} \mathcal{H} \mathcal{N}^{-1/2}]_{\nu\nu}^{K'K}(\rho', \rho)$ is the orthogonalized kernel obtained from the Hamiltonian and overlap (or norm) matrix elements

$$\mathcal{H}_{\nu\nu}^{J^{\pi T}}(x', y', x, y) = \langle \Phi_{\nu x' y'}^{J^{\pi T}} | \hat{\mathcal{A}}_\nu H \hat{\mathcal{A}}_\nu | \Phi_{\nu xy}^{J^{\pi T}} \rangle, \quad (5)$$

$$\mathcal{N}_{\nu\nu}^{J^{\pi T}}(x', y', x, y) = \langle \Phi_{\nu x' y'}^{J^{\pi T}} | \hat{\mathcal{A}}_\nu \hat{\mathcal{A}}_\nu | \Phi_{\nu xy}^{J^{\pi T}} \rangle, \quad (6)$$

after projection over the basis $\phi_K^{\ell_x \ell_y}(\alpha)$, and E is the total energy. Equation (4) is solved with either bound- or genuinely three-body scattering-state (i.e., no bound two-body subsystems are present) boundary conditions by means of the microscopic R -matrix method on a Lagrange mesh [15–19]. For more details on the three-cluster NCSM/RGM formalism, we refer the interested reader to Ref. [14], where we first applied the approach to the description of the ground state of ${}^6\text{He}$ within a ${}^4\text{He} +$

$n + n$ basis ($a_2, a_3 = 1$). Here, we apply the same framework to the much more challenging problem of the continuum of this system, for which the hyper-radial wave function behaves asymptotically as $u_{\nu K}^{J^{\pi T}}(\rho) \propto [H_K^-(\kappa\rho) \delta_{\nu\nu'} \delta_{KK'} - S_{\nu K, \nu' K'} H_K^+(\kappa\rho)]$ (with H_K^\pm being the incoming and outgoing functions for neutral systems [20], κ the wave number, and S the three-body scattering matrix of the process). First, we present our results and compare them to experiment. A discussion of the uncertainty of our calculations as it relates to the convergence with respect to the adopted model space will follow.

Results.—The present calculations are based on the chiral next-to-next-to-next-to-leading order ($N^3\text{LO}$) NN [21] interaction softened via the similarity renormalization group (SRG) to minimize the influence of momenta higher than $\Lambda = 1.5 \text{ fm}^{-1}$. This soft potential permits us to reach convergence in the HO expansions within $N_{\text{max}} \sim 13$ quanta, the largest model space presently achievable. At the same time, it also leads to a ${}^4\text{He}$ g.s. energy [22,23] and $n + {}^4\text{He}$ phase shifts [24] close to experiment despite the omission of three-nucleon ($3N$) forces, which are beyond the scope of this first *ab initio* study of the ${}^4\text{He} + n + n$ continuum.

We further describe the ${}^4\text{He}$ cluster only by its $I_1^{\pi_1} T_1 = 0^+0$ g.s. and ignore core polarization effects, which have been estimated to account for $\sim 5\%$ of the ${}^6\text{He}$ binding energy [14]. The inclusion of excited states of the core leads to a (presently) unbearable increment of the computational size of the problem. This will be overcome in the future by coupling the present three-cluster model space with eigenstates of the six-body system within the no-core shell model with continuum [25,26].

We solve Eq. (4) for the $J^\pi = 0^\pm, 1^\pm, 2^\pm$ channels and extract the corresponding phase shifts from the diagonal elements of the three-body scattering matrix or from its diagonalization, when large off-diagonal couplings are present. A summary of the obtained low-lying attractive eigenphase shifts is presented in Fig. 1. We have identified several resonances. The lowest and sharpest appears in the 2^+ channel around 1.25 MeV above the ${}^4\text{He} + n + n$ threshold. An analysis of this resonance, corresponding to the very well-known first excited state of ${}^6\text{He}$, shows that it is dominated by 1S_0 neutrons in an $\ell_y = 2$ relative motion with respect to the ${}^4\text{He}$ g.s. ($S, \ell_x = 0; L, \ell_y, K = 2$). A second broader 2^+ resonance emerges at ~ 2.6 MeV, where the prevalent picture is that of the halo neutrons with aligned spins, moving relative to each other and to the core in P wave ($S, \ell_x, L, \ell_y = 1; K = 2$). The same structure also characterizes a 1^+ resonance located at slightly higher energy. Resonances also appear in the 2^- and 0^- channels, dominated by $S, \ell_x, L = 1$ and $\ell_y = 0$ quantum numbers. On the other hand, the rapid growth through 90° characteristic of a resonance is not present in the 1^- or in the 0^- channels. Therefore, we cannot see any evidence of a low-lying state that could be identified with the 1^- soft dipole

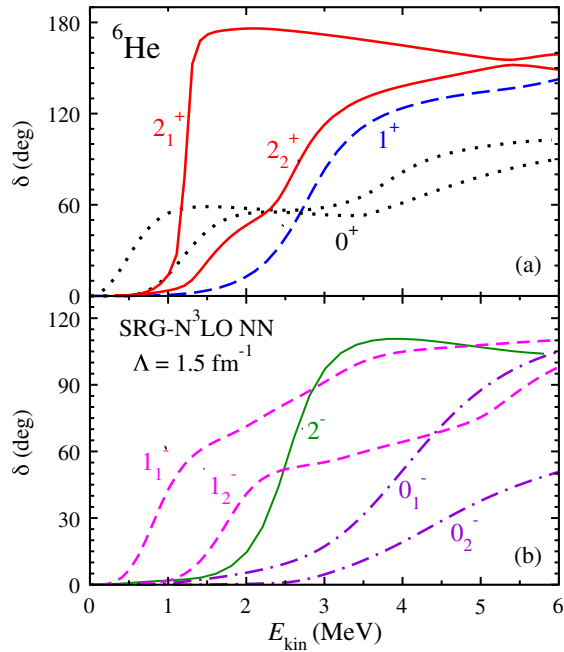


FIG. 1 (color online). Calculated ${}^4\text{He} + n + n$ (a) positive- and (b) negative-parity attractive eigenphase shifts as a function of the kinetic energy E_{kin} with respect to the two-neutron emission threshold. See the text for further details.

mode suggested in Refs. [1,3]. In addition, our results do not support the presence of a low-lying 0^+ monopole resonance above the 1^+ state reported by previous theoretical investigations of the ${}^4\text{He} + n + n$ continuum, in which the ${}^4\text{He}$ was considered as an inert particle with no structure. These three-body calculations, performed within the hyperspherical-harmonics basis [8,9,20,27] and with the complex scaling method [28,29], obtained a similar sequence of 2_1^+ , 2_2^+ , 1^+ , and 0_2^+ levels, but different resonance positions and widths. (Only the first two 2^+ resonances were shown in Ref. [20].) Microscopic ${}^4\text{He} + n + n$ calculations based on schematic interactions were later reported in Refs. [10,11] but showed only results for the 2_1^+ narrow resonance and do not comment on a 0^+ excited state.

In Fig. 2, the energy spectrum of states extracted from the resonances of Fig. 1 is compared to the one recently measured at GANIL [4]. Our results are consistent with the presence of the second low-lying narrow 2^+ resonance observed for the first time in this experiment. A $J = 1$ resonance was also measured at 4.3 MeV; however, the parity of such a state is not yet determined, and it is not possible to univocally identify it with the 1^+ resonance found at 2.77 MeV in the present calculations. At the same time, the energy dependence of the 1^- eigenphase shifts of Fig. 1(b) does not favor the interpretation of this low-lying state as a dipole mode. We also predict two broader negative-parity states not observed.

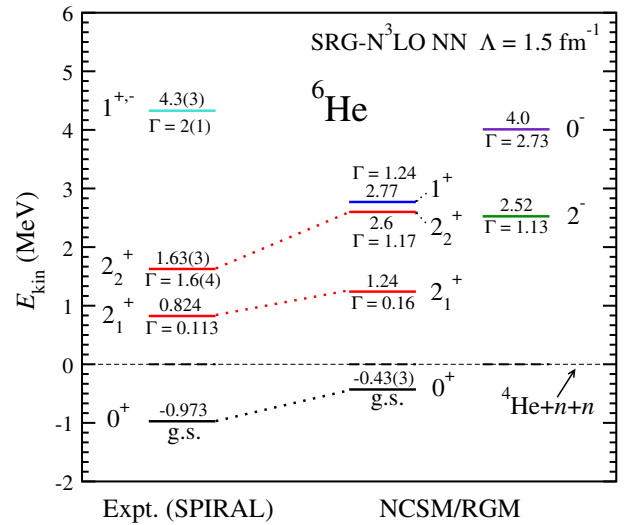


FIG. 2 (color online). Comparison of the spectrum obtained within this work using the NCSM/RGM to the experimental spectrum measured at the SPIRAL facility (GANIL) [4].

A thorough study of the convergence of the results with respect to all parameters defining the size of our model space was performed. These are the maximum value K_{max} of the hyperangular momentum in the expansion (3), the size N_{max} of the HO basis used to calculate the g.s. of ${}^4\text{He}$ and the localized parts of Eqs. (5) and (6), and finally, the size $N_{\text{ext}} \gg N_{\text{max}}$ of the extended HO basis used to represent a delta function in the core-halo distance entering the portion of the Hamiltonian kernel that accounts for the interaction between the halo neutrons (see Eq. (39) of Ref. [14]). In each case, the number of integration points and the hyper-radius a used to match internal and asymptotic solutions within the R -matrix method on the Lagrange mesh were chosen large enough to reach stable, a -independent results. All calculations were performed with the same $\hbar\Omega = 14$ MeV frequency adopted for the study of the ${}^6\text{He}$ g.s. [14].

We first set the extended HO basis size to the value ($N_{\text{ext}} = 70$) we found to be sufficient for the 0^+ g.s. energy [14] and established that expansion (3) converges at $K_{\text{max}} = 19/20$ for all negative- or positive-parity channels except the 0^+ , requiring $K_{\text{max}} = 28$. Examples of the convergence pattern with respect to the HO basis size N_{max} are shown in Fig. 3. In general, convergence is satisfactory at $N_{\text{max}} = 13$. For the higher-lying resonances, this value is not quite sufficient but already provides the qualitative behavior to start discussing the continuum structure of the system. Next, we study the dependence on N_{ext} , which regulates the range of the potential kernel. Not unexpectedly, an increase of N_{ext} requires at the same time incrementing the matching hyper-radius a needed to reach the asymptotic region (we used values of up to 60 fm) and K_{max} , for which we used values as high as 40 in the 0^+

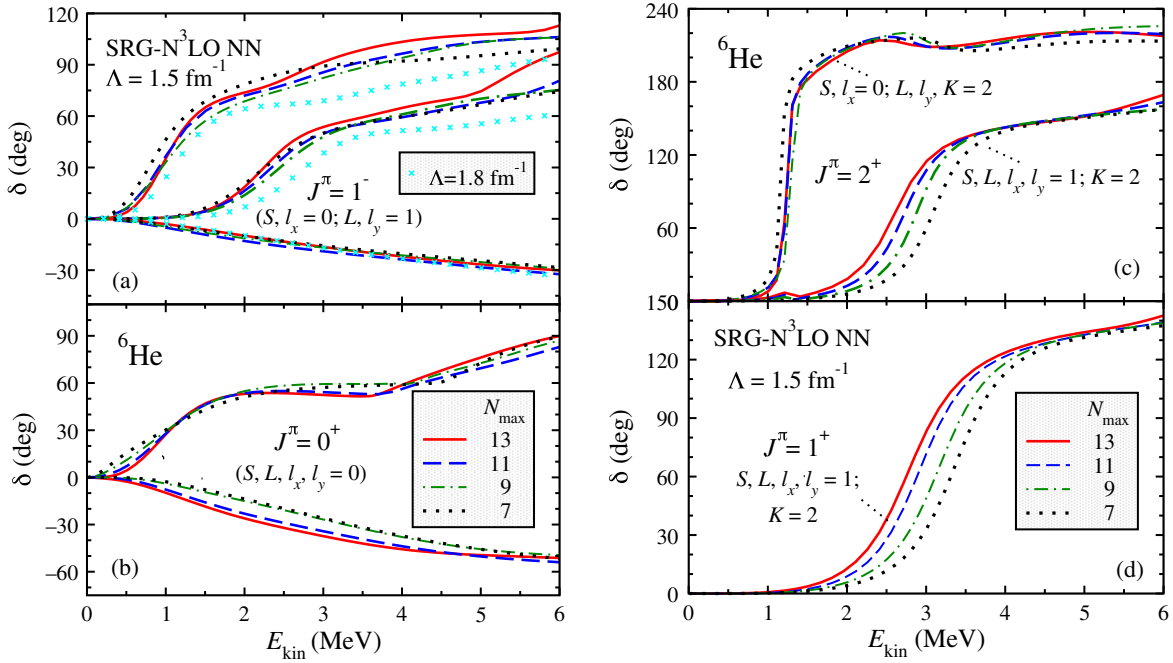


FIG. 3 (color online). Convergence behavior of calculated ${}^4\text{He} + n + n$ (a) $J^\pi = 1^-$ and (b) 0^+ eigenphase shifts at $K_{\text{max}} = 19$ and 28, respectively, and (c) 2^+ and (d) 1^+ diagonal phase shifts at $K_{\text{max}} = 20$ with respect to the size N_{max} of the NCSM/RGM model space for the SRG $N^3\text{LO } NN$ potential with $\Lambda = 1.5 \text{ fm}^{-1}$. For these calculations, we used an extended HO model space of $N_{\text{ext}} = 70$ and a matching radius of $a = 30 \text{ fm}$. In (a), 1^- phase shifts obtained with the $\Lambda = 1.8 \text{ fm}^{-1}$ SRG NN potential at $N_{\text{max}} = 11$ are also shown for comparison. When presenting eigenphase shifts on (a) and (b), the quantum numbers of the dominant components are shown in parentheses. These have been identified by comparing the eigenphase shifts with the diagonal phase shifts.

channel. This limited the maximum value of N_{ext} used to obtain our best ($N_{\text{max}} = 13$) results for the 0^+ , 1^- , and 2^+ results of Figs. 1 and 2 to 200, 110, and 90, respectively. As shown in Fig. 4, the influence of N_{ext} is most pronounced for attractive phase shifts in which the two neutrons are in 1S_0 relative motion. There, the matrix elements of the nn interaction from which the potential kernel is built (see Eq. (39) of Ref. [14]) tend to be large. By far, the dominating effect is the steeper onset of the 0^+ attractive eigenphase shifts that, as already noted in Ref. [20], becomes more accentuated for (higher-lying) components with $K > 0$. However, the qualitative results remain unchanged. In particular, the value of N_{ext} has little or no influence on the position and width of the resonances. Also, the binding energy of the 0^+ ground state of ${}^6\text{He}$ calculated in Ref. [14] remains unchanged within this much larger model space. Finally, changing the value of the SRG parameter used to soften the NN interaction to $\Lambda = 1.8 \text{ fm}^{-1}$ does not change the overall structure of the continuum states. Bearing in mind that, with this harder potential, convergence is slower, in each channel, we obtain the same number of resonances with similar widths, although somewhat shifted in energy (less than 1 MeV), as shown in Fig. 3 for the 1^- . This is evidence that the softness of the potential used is not introducing any spurious resonances and, therefore, verifies the reliability of our results.

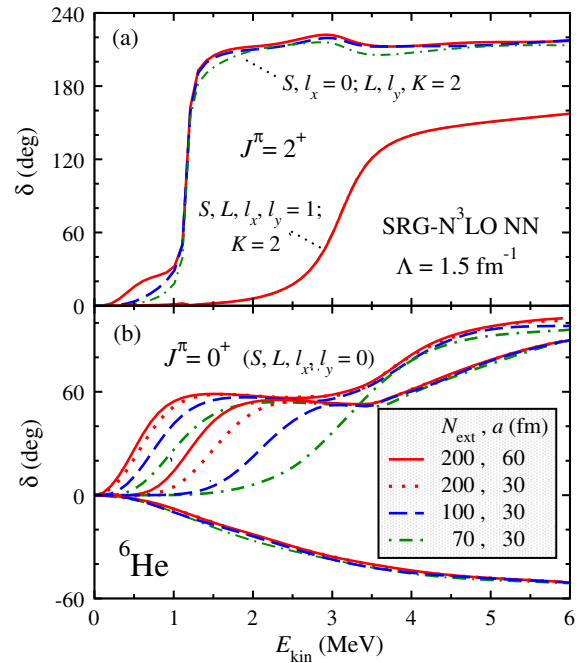


FIG. 4 (color online). Dependence on the size of the extended HO model space N_{ext} of calculated ${}^4\text{He} + n + n$ (a) $J^\pi = 2^+$ diagonal phase shifts corresponding to the 2_1^+ and 2_2^+ resonances at $N_{\text{max}} = 7$ and (b) the first three eigenphase shifts for the $J^\pi = 0^+$ channel at $N_{\text{max}} = 13$. The curves overlap for the 2_2^+ resonance in (a).

Conclusions.—We calculated, for the first time within an *ab initio* approach, the continuum spectrum of ${}^6\text{He}$ as a ${}^4\text{He} + n + n$ system. Given the low two-neutron separation energy of this nucleus, including the three-cluster basis in the calculation is essential. We found several resonances, including the well-known narrow 2_1^+ and the recently measured broader 2_2^+ . Additional resonant states emerged in the 2^- and 1^+ channels near the second 2^+ resonance and in the 0^- at slightly higher energy. We found no evidence of low-lying resonances in the 0^+ and 1^- channels. Therefore, our results do not support the idea that the accumulation of dipole strength at low energy is originated by a three-body 1^- resonance.

The inclusion of $3N$ forces and core polarization effects through the coupling of ${}^6\text{He}$ eigenstates within the no-core shell model with continuum are underway and will increase the predictive capability of the method. Finally, we expect that complementing this approach with the use of two integral relations derived from the Kohn variational principle [30–32] will increase the range of systems that can be described by limiting the distance for which the wave function has to be calculated. This will be essential for the study of ${}^{11}\text{Li}$ within a ${}^9\text{Li} + n + n$ basis.

Computing support for this work came from the LLNL institutional Computing Grand Challenge Program and from an INCITE Award on the Titan supercomputer of the Oak Ridge Leadership Computing Facility (OLCF) at ORNL. We thank the Institute for Nuclear Theory at the University of Washington for its hospitality and the Department of Energy for partial support during the completion of this work. This work was prepared in part by LLNL under Contract No. DE-AC52-07NA27344. Support from the NSERC Grant No. 401945-2011 and U.S. DOE/SC/NP (Work Proposal No. SCW1158) is acknowledged. TRIUMF receives funding via a contribution through the Canadian National Research Council.

* cromeroredondo@triumf.ca

† quaglioni1@llnl.gov

‡ navratil@triumf.ca

§ hupin1@llnl.gov

- [1] S. Nakayama, T. Yamagata, H. Akimune, I. Daito, H. Fujimura, Y. Fujita, M. Fujiwara, K. Fushimi, T. Inomata, H. Kohri, N. Koori, K. Takahisa, A. Tamii, M. Tanaka, and H. Toyokawa, *Phys. Rev. Lett.* **85**, 262 (2000).
- [2] J. Jänecke, T. Annakkage, G. P. A. Berg, B. A. Brown, J. A. Brown, G. Crawley, S. Danczyk, M. Fujiwara, D. J. Mercer, K. Pham, D. A. Roberts, J. Stasko, J. S. Winfield, and G. H. Yoo, *Phys. Rev. C* **54**, 1070 (1996).
- [3] T. Nakamura, T. Aumann, D. Bazin, Y. Blumenfeld, B. A. Brown, J. Caggiano, R. Clement, T. Glasmacher, P. A. Lofy, A. Navin, B. V. Pritychenko, B. M. Sherrill, and J. Yurkon, *Phys. Lett. B* **493**, 209 (2000).
- [4] X. Mougeot, V. Lapoux, W. Mittig, N. Alamanos, F. Auger, B. Avez, D. Beaumel, Y. Blumenfeld, R. Dayras, A. Drouart, C. Force, L. Gaudefroy, A. Gillibert, J. Guillot, H. Iwasaki, T. A. Kalanee, N. Keeley, L. Nalpas, E. C. Pollacco, T. Roger *et al.*, *Phys. Lett. B* **718**, 441 (2012).
- [5] P. Navrátil, J. P. Vary, W. E. Ormand, and B. R. Barrett, *Phys. Rev. Lett.* **87**, 172502 (2001).
- [6] P. Navrátil and W. E. Ormand, *Phys. Rev. C* **68**, 034305 (2003).
- [7] S. C. Pieper, R. B. Wiringa, and J. Carlson, *Phys. Rev. C* **70**, 054325 (2004).
- [8] B. V. Danilin, T. Rogde, S. N. Ershov, H. Heiberg-Andersen, J. S. Vaagen, I. J. Thompson, and M. V. Zhukov, *Phys. Rev. C* **55**, R577 (1997).
- [9] B. V. Danilin, I. J. Thompson, J. S. Vaagen, and M. V. Zhukov, *Nucl. Phys.* **A632**, 383 (1998).
- [10] S. Korennov and P. Descouvemont, *Nucl. Phys.* **A740**, 249 (2004).
- [11] A. Damman and P. Descouvemont, *Phys. Rev. C* **80**, 044310 (2009).
- [12] G. Hagen, M. Hjorth-Jensen, and J. S. Vaagen, *Phys. Rev. C* **71**, 044314 (2005).
- [13] T. Myo, K. Katō, and K. Ikeda, *Phys. Rev. C* **76**, 054309 (2007).
- [14] S. Quaglioni, C. Romero-Redondo, and P. Navrátil, *Phys. Rev. C* **88**, 034320 (2013).
- [15] D. Baye, J. Goldbeter, and J.-M. Sparenberg, *Phys. Rev. A* **65**, 052710 (2002).
- [16] D. Baye, M. Hesse, J.-M. Sparenberg, and M. Vincke, *J. Phys. B* **31**, 3439 (1998).
- [17] M. Hesse, J. Roland, and D. Baye, *Nucl. Phys.* **A709**, 184 (2002).
- [18] M. Hesse, J.-M. Sparenberg, F. V. Raemdonck, and D. Baye, *Nucl. Phys.* **A640**, 37 (1998).
- [19] P. Descouvemont, C. Daniel, and D. Baye, *Phys. Rev. C* **67**, 044309 (2003).
- [20] P. Descouvemont, E. M. Tursunov, and D. Baye, *Nucl. Phys.* **A765**, 370 (2006).
- [21] D. R. Entem and R. Machleidt, *Phys. Rev. C* **68**, 041001 (2003).
- [22] E. D. Jurgenson, P. Navrátil, and R. J. Furnstahl, *Phys. Rev. Lett.* **103**, 082501 (2009).
- [23] E. D. Jurgenson, P. Navrátil, and R. J. Furnstahl, *Phys. Rev. C* **83**, 034301 (2011).
- [24] P. Navrátil and S. Quaglioni, *Phys. Rev. Lett.* **108**, 042503 (2012).
- [25] S. Baroni, P. Navrátil, and S. Quaglioni, *Phys. Rev. Lett.* **110**, 022505 (2013).
- [26] S. Baroni, P. Navrátil, and S. Quaglioni, *Phys. Rev. C* **87**, 034326 (2013).
- [27] S. N. Ershov, T. Rogde, B. V. Danilin, J. S. Vaagen, I. J. Thompson, and F. A. Gareev (Russian-Nordic-British Theory (RNBT) Collaboration), *Phys. Rev. C* **56**, 1483 (1997).
- [28] K. K. S. Aoyama, S. Mukai, and K. Ikeda, *Prog. Theor. Phys.* **94**, 343 (1995).
- [29] K. K. S. Aoyama, S. Mukai, and K. Ikeda, *Prog. Theor. Phys.* **93**, 99 (1995).
- [30] P. Barletta, C. Romero-Redondo, A. Kievsky, M. Viviani, and E. Garrido, *Phys. Rev. Lett.* **103**, 090402 (2009).
- [31] C. Romero-Redondo, E. Garrido, P. Barletta, A. Kievsky, and M. Viviani, *Phys. Rev. A* **83**, 022705 (2011).
- [32] A. Kievsky, M. Viviani, P. Barletta, C. Romero-Redondo, and E. Garrido, *Phys. Rev. C* **81**, 034002 (2010).